

Analysis of short crack growth from microscopic fatigue properties

X.D. Li ^{*}, L. Edwards

Fracture Research Group, Materials Discipline, Faculty of Technology, The Open University, Milton Keynes, MK7 6AA, UK

Abstract

Successful simulation of kinetics of small fatigue crack growth entails three aspects: Stage I, Stage II growth rate prediction and transition prediction. In this paper attention is focused on growth rate predictions. By using microstructurally-affected-zone and process zone concepts, microscopic fatigue behaviour of small fatigue crack propagation is logically linked with macroscopic fatigue behaviour, showing an intrinsic relation between small fatigue crack growth and macroscopic low-cycle fatigue properties during crack growth. Furthermore, variation of relatively big plastic zone size associated with a growing small fatigue crack is kinetically simulated. As a result a quantitative prediction model of growth rates for Stage I and Stage II growth has been developed whose explicit advantage is that the growth rate of small fatigue crack can now be predicted in terms of bulk fatigue properties in conjunction with local microstructural characteristics.

1. Introduction

Small fatigue crack in aluminium alloys has been well classified into microstructurally small fatigue crack and physically small fatigue crack. Small fatigue cracks may initiate directly either at slip bands in matrix as a result of dislocation motion or at a particle bonded in matrix due to stress concentration. Wherever a small fatigue crack initiates it may experience two stages of growth [1]. In Stage I growth there are two prominent features associated with the small fatigue crack growth: shear mechanism primarily dominates the propagation of the small crack; and local microstructure has a significant effect on the growth of small fatigue crack. This influ-

ence of local microstructure cannot be negligible until the growth mode of shear mechanism completely shifts to tension mechanism. In Stage II growth small fatigue crack growth is still affected to some degree by the local microstructure. However, the propagation of small fatigue crack is considered to be different; it is primarily governed by tension mechanism and there is no longer a strong dependence of propagation upon the local microstructure because the metallurgical influence of local microstructure on fatigue crack growth is averaged. Thus, the mechanics of continuum may be applicable. Furthermore, with the increase of small fatigue crack length up to such a degree free from influence of surface effect, the growth is inevitable to be in compliance with the bulk fatigue behaviour. This implies that there exists a coherent connection of fatigue growth with bulk fatigue properties, in other

^{*} Corresponding author. Tel. +44 908 653977, fax +44 908 653858, e-mail X.D. Li@open.ac.uk.

words, a connection between micro-growth of small fatigue crack and macro-fatigue behaviour.

Although there have been a number of models proposed to predict growth rate of small fatigue crack, their general application to fatigue life prediction requires the determination of an expression for crack growth, which is obtained from careful and tedious characterisation of small fatigue cracks. Particularly, the metallurgical characteristics of polycrystalline material in relation to small fatigue crack growth has not been modelled yet. The coherent connection of micro-growth of small fatigue crack with macro-fatigue behaviour is still something unclear. As a result of theoretical study and experimental observations, we are trying to physically model a kinetic relation between metallurgical characteristics of material and characteristics of small fatigue crack tip during crack growth, and hence to make a connection of micro-fatigue with macro-fatigue. A kinetic variation of plastic zone in the process of fatigue crack propagation is also simulated with emphasis on the variation of the ratio of plastic zone size to small crack length. This simulation is totally based on experimental results of plastic zone measurement along with elastic-plastic fracture mechanics. In general, we are trying to establish a general model for aluminium alloys that can predict growth rate by means of conventional low-cycle fatigue properties without tedious crack length measurements and can simulate the kinetic evolution of small fatigue crack growth.

2. Background of modelling

2.1. Simulation of microstructure for polycrystalline materials

Microstructure has a dramatic influence on small fatigue crack, particularly on its propagation of early stage. Since a growing small fatigue crack is controlled to some extent by local microstructure, it seems to us that local microstructure should be modelled. However, it is impossible to simulate each local effect of single metallurgical feature, such as grain size, grain orientation etc., on propagation of small fatigue crack. What is known is that it is possible to take the microstructure effect into account by defining an appropriate microstructural dimension. Proposed is a concept of microstructurally-affected-zone that is in front of a small fatigue crack tip to represent local metallurgical features. Its size can be taken as an appropriate microstructural dimension to measure the effect of local microstructure. Now the question is how to relate this microstructurally-affected-zone to a physical quantity and determine it quantitatively.

Based on a microscale observation of a real material, it was stated in [1] that “the microstructural features in metals cause break up of the crack front into segments that are related to elementary blocks operating with some degree of independence from their neighbours but under the general influence of macroscopic crack of which they are a part”. Following this concept a

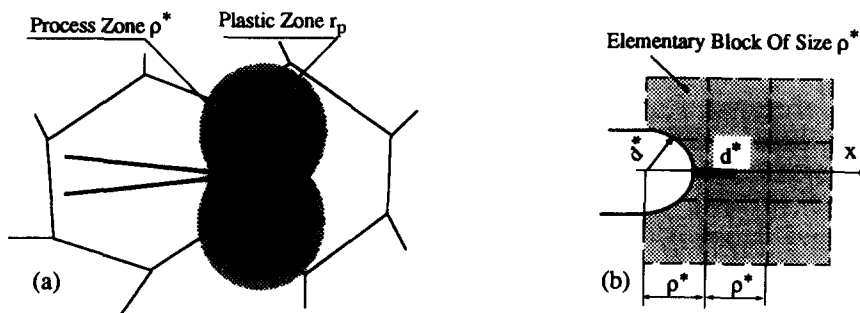


Fig. 1. Schematic representation of (a) elementary block and (b) tip characteristic of a small fatigue crack.

real aluminium alloy is conceived to be composed of elementary blocks of finite linear dimension ρ^* . The elementary blocks divide the material into segments and are identical in size. Since a surface small fatigue crack propagates across elementary blocks, we can naturally and reasonably associate the elementary block size with the microstructurally-affected-zone size as if a real aluminium alloy would be zoned by microstructurally-affected-zone. Furthermore, the microstructurally-affected-zone size is taken as a measure to be in accordance with the elementary block size. Therefore, any effect of local microstructure on a growing small fatigue crack is thought to be reachable via each elementary block/microstructurally-affected-zone. With such a simulation we are able to equate the microstructurally-affected-zone size to a simplified physical quantity, i.e., the elementary block size. Fig. 1 provides a schematic representation of elementary blocks along with crack tip configuration.

2.2. Representation of small fatigue crack tip

Consider a physically small fatigue crack that lies in an infinite body subjected to a uniform tension stress (see Appendix A). No matter how small a crack tip is, it is still valid to characterise a small crack tip as surrounded by a plastic zone and a so called process zone just ahead of the crack tip to avoid stress/strain singularity there. The process zone is physically defined to be dependent upon the plastically deformed zone and local microstructure, such as grain size. Naturally, the process zone size d^* and the plastic zone size r_p are mostly concerned.

However, the small fatigue crack tip compared with relative large elementary blocks is still smaller. The behaviour of crack tip is believed to be controlled by localised driving force in a smaller zone at the crack tip. The stress/strain distribution varies throughout cracked blocks so the uniform stress/strain contributing to localised driving force for small fatigue crack propagation is considered to occur only within the process zone just ahead of the crack tip. This assumption is obviously objective because the

process zone is defined at a small fatigue crack tip within a very small region (smaller than the plastic zone) to avoid stress singularity at the crack tip. The process zone size d^* varies, increasing all the way in the process of small fatigue crack propagation as the plastic zone size does. An incremental advance of length d^* is associated with a local measure of fatigue damage that controls fatigue crack growth. Since the total increment d^* of crack length is a direct result of fatigue cycles necessary to fracture material of size d^* in front of the growing small fatigue crack, the crack growth rate at any time will be therefore given by the process zone size divided by its fatigue damage "life", which can be measured quantitatively by the ratio

$$\frac{da}{dN} = \frac{d^*}{N_f}. \quad (1)$$

3. Description of modelling process for stage II small fatigue crack

It has been modelled already that small fatigue crack propagation is the result of successive cracking over the distance d^* . This cracking process can be regarded as strain controlled fatigue in the process zone and hence the fatigue cycles can be determined in terms of Coffin–Manson relation. In this respect local plastic strain in the process zone significantly contributes to the driving force for crack growth. It is the localised inelastic strain that actually controls small fatigue crack propagation and, therefore the fatigue life. In addition, most polycrystalline materials can be treated as isotropic continuum. Therefore, free surface effect due to local unusual isotropic (or anisotropic) dislocations [2] on early stage growth of small fatigue crack is put aside in the modelling for the time being.

3.1. Strain calculation at small fatigue crack tip

Consider a microcrack of length $2a$ that lies in an infinite body subjected to uniform tension loading. The microcrack has a similar configura-

tion of quasi-ellipse whose semi-major axis takes value a . Because of its being small, the microcrack can be mathematically treated as a “line crack”. The displacement of this line crack in an infinite sheet under uniaxial tension stress σ are given for plane strain condition by the relation [3]

$$v = (1 - \nu^2) \sigma a \left(\frac{\sin \theta}{E} \right), \quad (2)$$

where a represents half surface crack length and θ is the angle between the point of interest and the major axis of the ellipse. After a forward loading the microcrack opens becoming a micronotch with blunted tip of radius d^* . In the meanwhile, a plastic zone of size r_p is formed as a result of applied loading at the micronotch tip. The opening displacement, δ , corresponding to this blunted surface micronotch can be evaluated (See Appendix A) by the following expression:

$$\delta = \frac{2(1 - \nu^2)}{E} (a + r_p) \left(1 - \left(\frac{x - a}{a + r_p} \right)^2 \right)^{1/2} \sigma. \quad (3)$$

To determine local strain at the microcrack tip we adopt a physical interpretation of crack tip blunting process made by others [4–6]. The microcrack tip blunts to a semi-circle of radius d^* without singularity of local strain at the tip. It has been theoretically established and practically employed [7,8] that the normal strain distribution in front of the microcrack tip along the major-axis takes a form of:

$$\varepsilon = \frac{\eta}{x - a} \quad (x > a), \quad (4)$$

where η is the deformation in a yielded zone just at the crack tip. In order to avoid strain singularity at $x = a$, we adopt an assumption as mentioned already that the deformation is held constant within the distance d^* from tip of the microcrack that has been named “process zone size”. If an elementary block of length ρ^* is initially elongated by $\delta/2$ in the forward loading, we should have

$$\varepsilon = \frac{\delta}{2\rho^* \omega}, \quad (5)$$

where ω is a triaxiality factor taking a value of 2.57 [9]. To meet the needs of continuity of Eq. (4) with relation to Eq. (5) at $x = a + d^*$, η must equal $\delta d^* / (2\rho^* \omega)$ leading to the following strain expression:

$$\varepsilon = \frac{\delta d^*}{2\rho^* \omega (x - a)}, \quad (6)$$

which scales strain distribution in front of the microcrack. Substituting Eq. (3) into Eq. (6), it yields an expression of strain distribution in front of the elliptical microcrack tip in the form of

$$\varepsilon = \frac{d^* (1 - \nu^2)}{\rho^* \omega E (x - a)} \left(1 + \frac{r_p}{a} \right) \times \left(1 - \left(\frac{\frac{x}{a} - 1}{1 + \frac{r_p}{a}} \right)^2 \right)^{1/2} \sigma a. \quad (7)$$

At $x = a + r_p$, it is a boundary between local elastic-plastic region and elastic region outside. The strain at this point can be determined by replacing x with $(a + r_p)$ in Eq. (7). With cyclic stress imposed on the infinite body, it is assumed that the cyclic strain distribution can be evaluated by means of Eq. (7) by replacing ε , σ with $\Delta\varepsilon/2$ and $\Delta\sigma/2$.

3.2. Kinetic simulation of plastic zone associated with a growing small fatigue crack

Plastic zone size associated with a small fatigue crack has been found to be another important physical quantity that plays an essential controlling role in small fatigue crack growth. Plastic deformation at a small crack tip dominates the local driving force around the crack tip. Unlike that of a long crack, the development of plastic zone of a small fatigue crack is very complicated due to local microstructure. It has been found that the plastic zone is likely to be truncated by grain boundaries due primarily to misorientation between neighbour grains when the small fatigue crack approaches a grain boundary [10,11]. A recent experimental measurement [10] on 7xxx aluminium alloys of plastic zone indicated that

the relatively large plastic zone corresponds to smaller crack length and the ratio of plastic zone size to crack length r_p/a initially decrease rapidly with increase of crack length and then decreases gradually until approaching a relatively stable value. This evolution follows a power function. On the other hand, it has been recognised that high ratio of applied stress to yield stress, σ_{\max}/σ_y , has a positive contribution to the comparatively large value of the ratio r_p/a [12,13] although some deforming grains are not entirely plastically deformed. Based on previous experimental measurements of plastic zone size as shown in literature [10,11], the evolution of this process with respect to small crack length and stress level is illustrated in Fig. 2 which shows a general decreasing trend of ratio r_p/a with increase of small fatigue crack length. Despite the fact that the plastic zone size corresponding to a given crack length may change in different aluminium alloys, it is believed that the evolution of the normalised plastic zone size r_p/a with respect to the crack length and the stress level may be approximately identical. However, this evolution of normalised plastic zone size is questionable when it is extended to very short crack size. This point is going to be addressed later.

As has been pointed out, a growing small crack

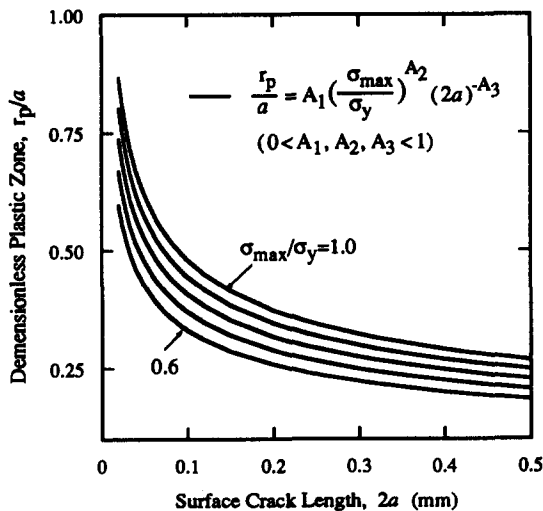


Fig. 2. An experimentally-determined evolution [10,11] of normalised plastic zone sizes for a growing small fatigue crack.

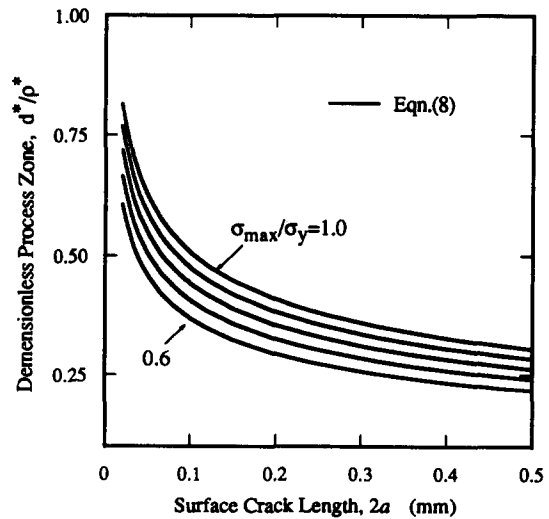


Fig. 3. Evolution of the normalised process zone size in conjunction with small fatigue crack length and microstructure.

is directly associated to the process zone just ahead of its tip. The defined process zone provides a linkage of blunting nature of the crack tip with each local elementary block but its size is under a general influence of plastic deformation at the microcrack tip. Once a small crack grows or its tip deflects, the process zone size changes simultaneously in compliance with local microstructure constraint, depending upon local plastic deformation and local microstructure. Owing to the known analytical expressions of Eqs. (2) to (7), use can be made of the requirement for strain equilibrium at the boundary between the elastic-plastic zone ahead of the microcrack tip and the elastic region outside. The strain at the boundary can be determined in terms of Eq. (7). The elastic strain just outside the elastic-plastic zone conforms to elastic field of the infinite body which can be directly derived in terms of partial differentiating with respect to Eq. (2), i.e., $(\partial v/\partial y)$ on the condition that the microcrack is so small that it can be regarded as a line crack. Consequently, we derived an analytical expression that revealed the evolution of this process zone size for a growing small crack as follows:

$$\frac{d^*}{\rho^*} = \frac{\omega}{2} \left(\frac{r_p}{a} \right) \left(1 + \frac{r_p}{a} \right)^{-0.5} \quad (8)$$

This analytical expression shows a coherent relation of process zone size d^* with microstructurally-affected-zone size ρ^* and the normalised plastic zone size r_p/a via stress ratio σ_{\max}/σ_y that makes it possible to link the microscopic fatigue behaviour of small fatigue crack propagation to macroscopic fatigue behaviour of bulk. The evolution of a normalised process zone size d^*/ρ^* is depicted in Fig. 3. It is also clear that the evolution of the normalised process zone size d^*/ρ^* illustrated in Fig. 3 has a similar pattern of that of the normalised plastic zone size r_p/a shown in Fig. 2. This consistence of pattern between evolution of the normalised plastic zone size r_p/a and that of the normalised process zone size d^*/ρ^* is not an occasional similarity but reveals and provides a mechanical basis indicating that the process zone size may be taken as a physical quantity to kinetically describe small fatigue crack, and hence is correlated with a small crack growth rate.

3.3. Coherent connection of growth rate with macroscopic fatigue properties

Successive cracking of the process zone over each elementary block results in crack extension. The inelastic strain within this process zone takes a primary contribution to local driving force at a small crack tip. Due to the localised nature of crack tip, the inelastic strain in the process zone is taken to be larger, comparing with elastic strain. The contribution of elastic strain can be ignored i.e. $\Delta\epsilon_p \approx \Delta\epsilon$. Now the local cyclic inelastic strain in the process zone can be theoretically determined by means of Eq. (7), letting $x = a + d^*$. This yields a microstructurally-related expression for local cyclic inelastic strain at the small fatigue crack tip

$$\frac{\Delta\epsilon_p}{2} = \frac{1 - \nu^2}{2\rho^* \omega E} \left(\left(1 + \frac{r_p}{a} \right)^2 - \left(\frac{d^*}{a} \right)^2 \right)^{0.5} \Delta\sigma a. \quad (9)$$

From the view point of continuum, any influence of local metallurgical features on small fatigue crack is not isolated to individually take effect but

generally is related in nature to macroscopic fatigue behaviour. This point lays a foundation in our modelling which makes it possible to link physically small fatigue crack growth to bulk fatigue behaviour. Since the failure of material element at crack tip is essentially due to strain-controlled fatigue, the fatigue cycles necessary to rupture the material element can be determined using conventional Coffin–Manson relation because relatively large plastic deformation does occur at a small fatigue crack tip [10–14]. The cyclic inelastic stress-strain response of aluminium alloys obeys a well-familiar power function, $\Delta\sigma/2 = K'(\Delta\epsilon_p/2)^{n'}$, in cyclic fatigue. A quantitative relation can be deduced to link fatigue cycles to failure to the local inelastic cyclic strain at the small crack tip in the form of

$$\frac{\Delta\epsilon_p}{2} = \left(\frac{(\sigma'_f - \sigma_m)\epsilon'_f}{K'} \right)^{1/1+n'} (2N_f)^{b+c/1+n'}, \quad (10)$$

where E is the Young modulus (MPa); K' the cyclic strength coefficient (MPa); n' the cyclic strain hardening exponent; N_f the fatigue cycles to failure; b and c the material constants involved in Coffin–Manson relation and σ_m , σ'_f , ϵ'_f stand for the mean stress level, fracture stress and fracture strain respectively. Making use of Eqs. (1), (9), (10), growth rate of a physically small fatigue crack can be given as

$$\begin{aligned} \frac{da}{dN} &= 2d^* \left(\left(\frac{K'}{(\sigma'_f - \sigma_m)\epsilon'_f} \right)^{1/1+n'} \frac{\Delta\epsilon_p}{2} \right)^{-(1+n')/b+c} \\ &= 2d^* \left(\left(\frac{K'}{(\sigma'_f - \sigma_m)\epsilon'_f} \right)^{1/1+n'} \frac{\Delta\epsilon_p}{2} \right)^{-(1+n')/b+c}. \end{aligned} \quad (11)$$

This is a growth law equation for a single physically small fatigue crack by which growth rate is predicted using conventional low-cycle fatigue properties and two proposed microscopic quantities, i.e., microstructurally-affected-zone size and process zone size. When stress level in Eq. (9) approaches fatigue limit $(\Delta\sigma)_{FL}$, Eq. (11) predicts a minimum growth rate. This equation is applicable to small fatigue cracks in Stage II propagation.

4. Modelling of Stage I growth rate

Classified in [1] are two stages of fatigue cracks growth no matter whether the crack initiates at slip bands or emanates from a particle. It was suggested that Stage I growth is similar to the process by which a crack is nucleated in an active slip band through the formation of a groove by unequal amounts of forward and reverse slip in neighbouring packets of slip planes. In Stage I a microcrack initiates and propagates in a crystallographic mode. Shear mode growth of the microcrack is attributed to the local damage due to strongly discrete glide edge dislocations at the crack tip. Crack propagation is governed by cyclic shear stress amplitude $\Delta\tau$. Barriers, such as grain boundaries, produce perturbations on the growth rate of small crack. Owing to a complex stress situation around a small fatigue crack tip, Stage I growth features a mixed mode propagation. Shear mechanism, however, is a primary one responsible for the Stage I growth. A theoretically developed alternative model of the blocking of dislocations at grain boundaries [15,16] provided a useful solution of plastic displacement to simulate the discontinuous character of slip transfer across grain boundaries. For edge dislocations and plane strain condition, the shear displacement at crack tip is given [15,16] by

$$\Delta\delta = \frac{4(1-\nu^2)}{E} \frac{\sqrt{1-n^2}}{n} \Delta\tau a, \quad (12)$$

where n is a normalised plastic zone size defined by $n = a/(a + r_p) = a/a_0$ for Stage I propagation. Once the plastic zone extends to each grain boundary the critical value n_c can be determined by [16]

$$n_c = \cos\left(\frac{\pi}{2} \left(\frac{\Delta\tau - \tau_{Li}}{\tau_{comp}}\right)\right) \quad (13)$$

where τ_{comp} is a comparison stress, $\tau_{Li} = \tau_{FL}/\sqrt{i}$ ($i = 1, 3, 5, \dots$) and τ_{FL} is a shear stress corresponding to fatigue limit as specified in [15,16].

Eq. (12) predicts a series of drops of growth rate because of barrier of grain boundaries [16] in the process of small fatigue crack growth. However, recent experimental observations [17,18] sig-

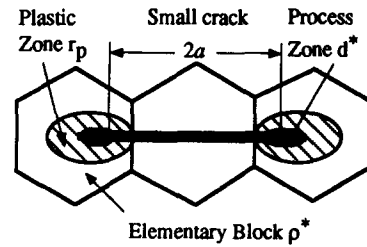


Fig. 4. Physical representation of shear crack analogue.

nify that first grain boundaries do not always cause drops of growth rate as a small fatigue crack penetrates it. Some grain boundaries take less effect of blockage to small fatigue crack growth. In other words, Eq. (12) may be valid for small fatigue crack propagation in the first few grains. The Stage I growth is considered to terminate at a transition crack length $2a_0$ at which the shear mechanism may shift to tension mechanism. Apparently, the prediction of growth rate in Stage I entails a determination of shear strain at the crack tip due to the gliding. Despite of different damage mechanisms possibly associated with the Stage I growth, we still adopt the concept of the process zone to configure the small fatigue crack tip as shown in Fig. 4. A growing small fatigue crack in this case is thus physically modelled as a micronotch with a tip radius of $(d^*)_0$ that is supposed to be equivalent to the process zone size associated with the transition crack length $2a_0$ and determined using Eq. (8). Applying Eq. (7) for the strain distribution in front of a micronotch, the cyclic shear strain can be approximately estimated in the form of

$$\Delta\gamma = \frac{\Delta\delta(d^*)_0}{2\rho^*\omega(x-a)}, \quad (14)$$

where ρ^* is still specified as the microstructurally-affected-zone size. Noting $\Delta\tau = \frac{1}{2}\Delta\sigma \sin[2(\pi/2) - \varphi]$ ($\varphi \cong 45^\circ$), the cyclic shear strain at $x = a + (d^*)_0$ can be rewritten in the form of

$$\frac{\Delta\gamma}{2} = \frac{(1-\nu^2) \sin\left[2\left(\frac{\pi}{2} - \varphi\right)\right] \sqrt{1-n^2}}{2\rho^*\omega E} \frac{\Delta\sigma a}{n} \quad (15)$$

A maximum shear strain theory [19] is used to estimate strain-controlled fatigue in the process zone and measure the fatigue resistance to maximum shear strain,

$$\frac{\Delta\gamma_{\max}}{2} = 1.30 \frac{\sigma'_f}{E} (2N_f)^b + 1.50 \epsilon'_f (2N_f)^c. \quad (16)$$

The valid use of Eq. (16) relies on the prerequisite that shear strain makes a major contribution to fatigue damage. By Eq. (16) the small crack growth rate is therefore simulated in terms of fatigue damage caused by the shear stress in the process zone. As a result, the growth rate law equation for a single small fatigue crack in shear mode takes the form of

$$\frac{da}{dN} = 2(d^*)_0 \left(\left(\frac{K'}{1.95(\sigma'_f - \sigma_m)\epsilon'_f} \right)^{1/1+n'} \times \frac{\Delta\gamma_{\max}}{2} \right)^{-(1+n')/b+c} \quad (17)$$

Eqs. (11) and (17) provide a unified model to predict growth rate of small fatigue cracks for both Stage II and Stage I propagation.

5. Predictions and discussions

In actual predictions of growth rates average grain size is initially used to represent the microstructurally-affected-zone size ρ^* to roughly take the microstructure effect into account. Regardless of applied stress levels, the stage I growth is considered to terminate at the first grain boundary and the transition from shear mechanism to tension mechanism is thought to start there. Fig. 5 illustrate a typical prediction of growth rate by using Eqs. (11) and (17), which are generally reasonable. However, in the transition regime at lower stress level, Eq. (17) predicts a constant transition crack length at which the growth rate is a minimum without stress effect. This is in contrast to physical intuition. Obviously, instead of average grain size, the microstructurally-affected-zone size ρ^* is a key parameter to be kinetically determined. It is possible to take a proper measure of the extent of the

influence of local microstructure. Recent study has shown that kinetic transition from Stage I to Stage II growth along with the microstructurally-affected-zone size can be analytically simulated [20]. Improved predictions of growth rate da/dN by the model are illustrated in Fig. 6 for 7075-T6 and 7150-T6 aluminium alloys.

The present model can predict the growth rate of physically small cracks completely, using macroscopic low-cycle fatigue properties via the process zone in conjunction with local microstructure, without any use of regression of experimental data. Among those fatigue properties (n' , K' , σ'_f , ϵ'_f , b , c) of aluminium alloys, the cyclic strain hardening exponent n' is typical because the change of growth rate is mainly dependent upon it. As the n' varies from unity to zero a polycrystalline material exhibits from a perfect plasticity to a perfect elasticity. However, it is hard to discriminate each individual effect of those physical quantities on small crack growth rate.

As described earlier, local microstructural dimension/elementary block has a significant influence over a growing small crack. Grain size is usually considered a factor to influence small crack growth. As a first step in modelling an average grain size is used to measure the mi-

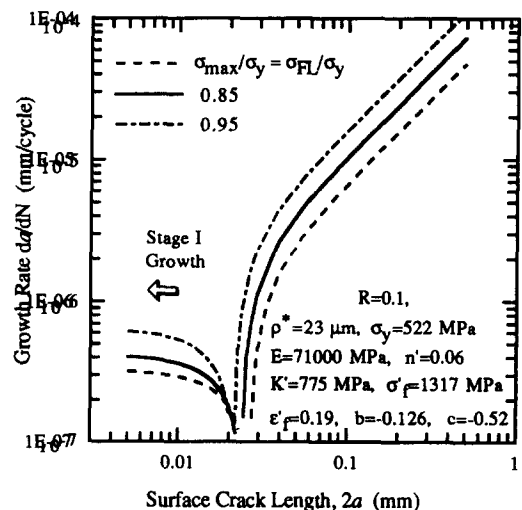


Fig. 5. Predictions of growth rates of small fatigue cracks by the developed model.

microstructure effect. Hence, the growth rate is directly associated with grain size. Experimental investigations to 7091 and 7050 [20] aluminium alloys have revealed that large grain did not result in fast growth of small cracks. A comparison of small crack growth rates for 2024, 2090, 6080, 7075, 7150, 7017 aluminium alloys with their grain sizes did not show a clear evidence of grain size dependence of small fatigue crack growth rate. It appears that the growth rate of small fatigue

crack is primarily controlled by the internal strength of grain boundaries together with local metallurgical features around the crack tip. Either grain boundary blocking or slip band orientation may cause decelerated (or accelerated) growth behaviour. Other obstacles bounded in matrix, such as inclusions or grain boundaries at subsurface, may also interfere with small crack growth causing deflection of the crack path or reducing growth rate. Therefore, it seems inade-

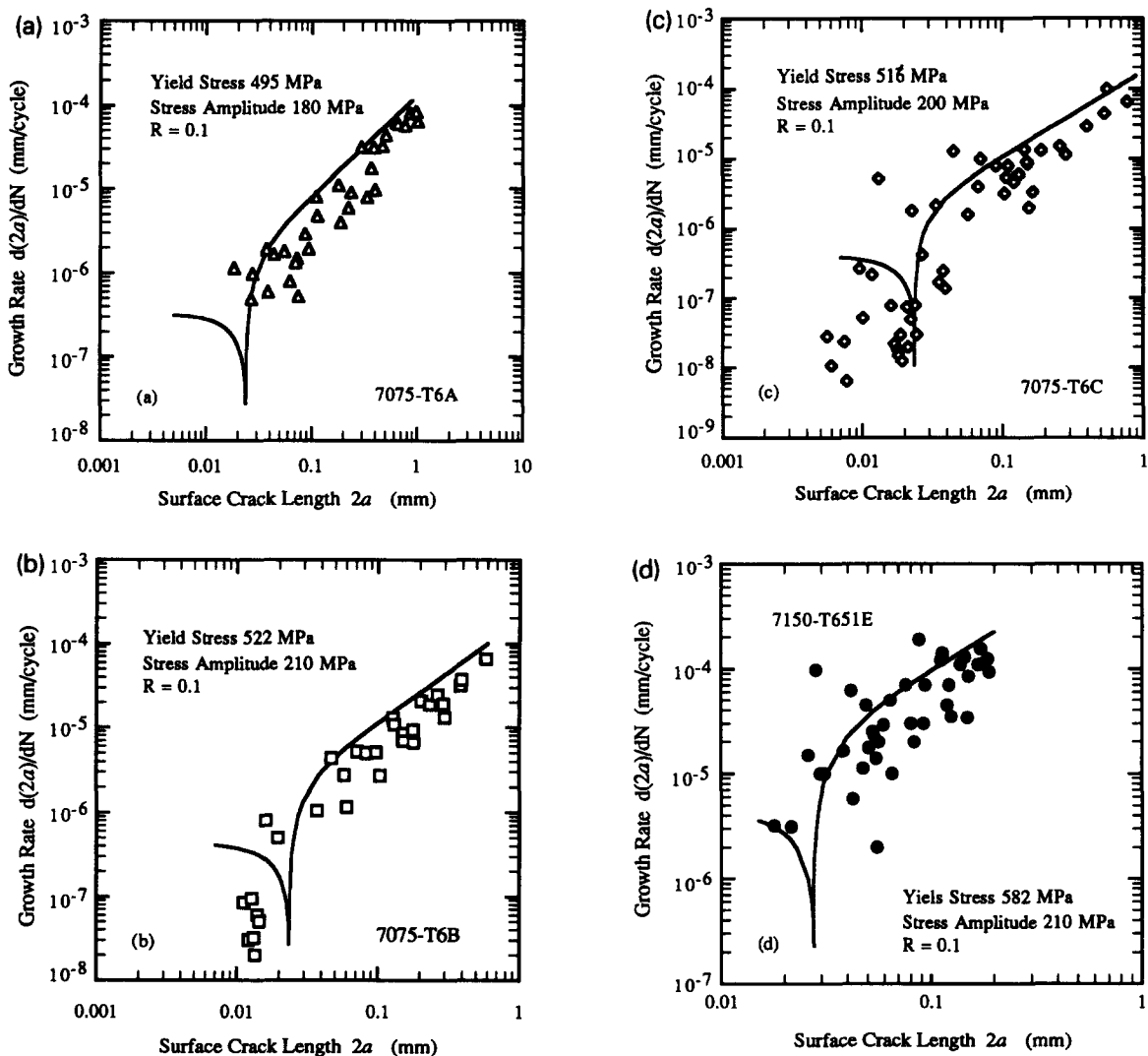


Fig. 6. Comparisons of predicted growth rates with experimental results [15] (a) 7075-T6A, (b) 7075-T6B, (c) 7075-T6C and (d) 7150-T6E.

quate to correlate the microstructural dimension ρ^* to an average grain size. Moreover, examination of measured data showed that the decrease of growth rate at first grain boundary was not always observed in experiment as it was expected by the grain boundary blockage mechanism. Instead, any grain boundary besides the first grain boundary may act as an effective barrier to severely deter propagation of small fatigue crack before the Stage I growth terminates. In this case a pile-up behaviour of dislocations ahead of a small fatigue crack tip as a result of blocking effect of grain boundary prevails if a small fatigue crack stems in a grain boundary. The blocking effect is particularly evident in the transition regime from Stage I to Stage II. The microstructurally-affected-zone size ρ^* should be determined by the transition condition rather than takes the average grain size. On the other hand, stress level is well known to influence small fatigue crack growth, particularly the transition from shear mechanism to tension mechanism.

Shear mechanism acting as a dominant mechanism in Stage I propagation takes long to conclude at lower stress level. This fact has been taken in account by means of defined process zone because the process zone size is strongly dependent upon stress level, plastic zone size and microstructurally-affected-zone size.

6. Conclusions

Early stage of small fatigue crack growth appears to be controlled to a great extent by microstructurally-affected-zone. The microstructurally-affected-zone acts as a bridge in the modelling across a gap between micro-fatigue behaviour and macro-fatigue behaviour although it is initially defined by taking an average measure of local microstructural features. Secondly, crack growth rate is predicted to increase with increase of stress level because high stress level causes a large plastic zone ahead of a small crack tip. As a result shear crack growth may terminate at a smaller crack length if applied stress level is higher. Contrarily, the period of shear crack growth may last long at lower stress levels. However, since the process zone size is determined either by plastic deformation or by local microstructure, it is still hard to discriminate which one of the two takes priority in early stage of propagation.

Using microstructurally-affected-zone and process zone concepts, a small fatigue crack tip is logically represented. Based on experimental investigations the evolution of plastic zone associated with a small fatigue crack is quantitatively evaluated which follows a decreasing pattern of power function during the small fatigue crack growth. The evolution of the normalised process zone size d^*/ρ^* is thus simulated in terms of the normalised plastic zone size r_p/a via the stress level in conjunction with the local microstructurally-affected-zone. As a result of modelling a quantitatively unified methodology for predicting growth rates of small fatigue cracks has been developed whose pronounced feature is that it reveals a coherent relation connecting small fatigue crack growth with bulk fatigue properties of

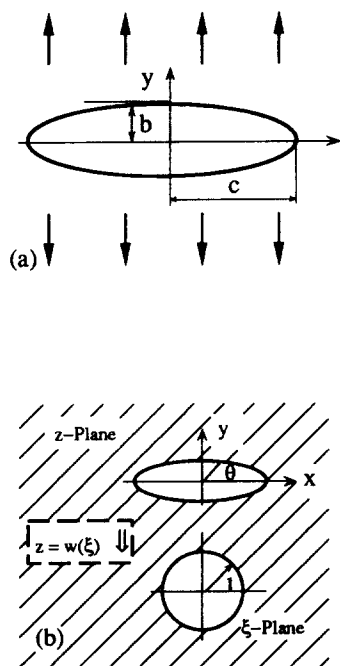


Fig. 7. (a) An elliptical crack in an infinite plate subjected to tension loading; (b) conformal mapping of an ellipse to a unit circle.

aluminium alloys, in other words, connecting the microscopic fatigue growth to the macroscopic bulk fatigue behaviour via the microstructurally-affected-zone. However, it seems inadequate to refer the microstructurally-affected-zone size ρ^* to any specific metallurgical size of aluminium alloys. The microstructurally-affected-zone size is related to a microstructurally-related condition that determines a transition from Stage I growth to Stage II growth.

Appendix A

Crack opening displacement derivation

Consider a quasi-ellipse contained in an infinite elastic body subjected to uniform uniaxial tensile stress (see Fig. 7(a)). The displacement function for this infinite body with an elliptical crack under uniaxial tension σ is given by the relation [3]

$$2\mu(u + iv) = \kappa\phi(z) - \overline{\phi'(z)} - \overline{\psi(z)}, \quad (18)$$

where u is the displacement in x -direction; v is the displacement in y -direction; $\mu = E/2(1 + \nu)$; $\kappa = (3 - \nu)/(1 + \nu)$ in plane stress and $\kappa = 3 - 4\nu$ in plane strain; $\phi(z)$ and $\psi(z)$ are the analytical complex functions. The solution of Eq. (18) is obtained by method of conformal mapping, transferring the ellipse in z -plane into a circle of unit radius in ξ -plane (see Fig. 7(b)) by the transformation

$$z = \omega(\xi) = A\left(\xi + \frac{M}{\xi}\right) \quad M < 1,$$

where $A = (c + b)/2$ and $M = (c - b)/(c + b)$; c and b being the semi-major and semi-minor axis of the ellipse respectively. After necessary transformation, Eq. (18) becomes

$$2\mu(u + iv) = \kappa\phi(\xi) - \omega(\xi)\overline{\phi'(\xi)/\omega'(\xi)} - \overline{\psi(\xi)}. \quad (19)$$

Above equality can be solved by letting [22]

$$\begin{aligned} \phi(\xi) &= \frac{\sigma A}{4} \left(\xi - \frac{2+M}{\xi} \right), \\ \psi(\xi) &= \frac{\sigma A}{2} \left(\frac{\xi^3 - (M^2 + 2M + 1)\xi - \xi^{-1}}{\xi^2 - M} \right), \end{aligned}$$

respectively. All complex functions, $\omega(\xi)$, $\phi(\xi)$, $\psi(\xi)$ and $\phi'(\xi)/\omega'(\xi)$, can be determined by taking $\xi = e^{i\theta}$ and substituting them into Eq. (19). The values of displacements can be calculated by separating the real part from imaginary part in Eq. (19) that is substituted. The imaginary parts in Eq. (19) is the displacement in y -direction. This displacement is expressed as,

$$v = \frac{\sigma A}{8\mu} \left(\frac{(3 - 5M + M^2 + M^3)(1 + \kappa) \sin \theta + 4(M^2 + 3M)(\kappa + 1) \sin^3 \theta}{1 - 2M + M^3 + 4M \sin^2 \theta} \right), \quad (20)$$

where θ is the angle between any point of interest along the ellipse face and the major axis of the ellipse. The crack opening displacement, δ , at any point of interest takes the value of $2v$. Under plane strain condition ($\kappa = 3 - 4\nu$), thus δ can be analytically expressed in the form of

$$\delta = \frac{\sigma A}{\mu} \left(\frac{(3 - 5M + M^2 + M^3)(1 - \nu) \sin \theta + 2(M^2 + 3M)(1 - \nu) \sin^3 \theta}{1 - 2M + M^3 + 4M \sin^2 \theta} \right). \quad (21)$$

Since crack is small it is reasonable to assume that this ellipse can be regarded as a "line crack". Thus c becomes the semi-crack length, a and $b \rightarrow 0$, consequently resulting in $M = 1$ and $A = a/2$. After these simplifications plus $x = a \cos \theta$, $\sin \theta = [1 - (x/a)^2]^{1/2}$ in (x, y) coordinate system, the crack opening displacement of this ellipse under plane strain condition ($\kappa = 3 - 4\nu$) can be calculated by

$$\delta = \frac{2(1 - \nu^2)}{E} \left(1 - \left(\frac{x}{a} \right)^2 \right)^{1/2} \sigma a. \quad (22)$$

Eq. (22) is similar with Westergaard's crack opening displacement equation. When plastic zone of size r_p , that is a distance from the crack tip to the edge of the plastic zone, is formed at this elliptical crack tip we considered an equivalent elastic elliptical crack whose tips in x -direction are located at the edge of the plastic zone. Therefore, δ is defined as the distance of separation of two faces of this equivalent crack due to its notional growth. The corresponding crack opening displacement of this equivalent crack is thus calculated by replacing a with $a + r_p$ in Eq. (22). However, since the crack is very small, the crack is actually embedded in a local plastically de-

formed region where the hypothesis of small scale yield is no longer applicable. Plenty of experimental research on notch-like crack [23–26] suggests that a crack mouth opening displacement (CMOP) may be adequate for a fully elastic-plastic condition to represent the actual crack tip opening displacement. For a surface small fatigue crack, take $x - a$ in Eq. (22) to determine the crack tip opening displacement.

References

- [1] P.J.E. Forsyth, *Proc. Of Crack Propagation Symp.*, Cranfield, The College of Aeronautics, Cranfield, UK (1962) pp. 76–94.
- [2] P.M. Hazzledink, *Defects, Fracture and Fatigue*, eds. B.A. Bilby, K.J. Miller and J.R. Willis (Cambridge University Press, 1984) pp. 384–399.
- [3] N.I. Muskhelishvili, *Some Basic Problems Of The Mathematical Theory Of Elasticity* (Noordhoff, Leiden, 1963).
- [4] D.N. Lai and V. Weiss, A notch analysis of fracture approach to fatigue crack propagation, *Metall. Trans. A* 9, 413–426 (1978).
- [5] J. Lantaigne and J.P. Bailon, Theoretical model for FCGR near the threshold, *Metall. Trans.* 12 A, 459–466 (1981).
- [6] G. Glinka, Accumulative model of fatigue crack growth, *Int. J. Fatigue* 4, 59–67 (1982).
- [7] T.R. Wilshaw, Deformation and fracture of mild steel Charpy specimens, *J. Iron Steel Inst.* 204, 936–942 (1966).
- [8] J.R. Rice and G.F. Rosengren, Plane strain deformation near a crack tip in a power-law hardening material, *J. Mech. Phys. Solids* 16, 1–12 (1968).
- [9] R. Hill, *The Mathematical Theory Of Plasticity*, First ed. (Oxford University Press, London, 1950) p. 248.
- [10] Y. Zhang and L. Edwards, The effect of grain boundaries on the development of plastic deformation ahead of small fatigue cracks, *Scripta Metallurgica et Materialia* 26, 1901–1906 (1992).
- [11] L. Edwards and Y.H. Zhang, Investigations of Small fatigue cracks – I. Plastic deformation associated with small fatigue cracks, *Acta Metall. Mater.* 42, 1413–1422 (1994).
- [12] K.S. Chan, and J. Lankford, A crack-tip strain model for the growth of small cracks, *Scripta Metallurgica et Materialia* 17, 529–532 (1983).
- [13] J. Lankford, D.L. Davidson and K.S. Chan, The influence of crack tip plasticity in the growth of small fatigue cracks, *Metall. Trans.* 15 A, 1579–1588 (1984).
- [14] Y. Zhang and L. Edwards, On the blocking effect of grain boundaries on small crystallographic fatigue crack growth, *Mater. Sci. Eng. A* 188 121–132 (1994).
- [15] A. Navarro and E.R. de los Rios, Short and long crack growth: a unified model, *Philos. Mag.* 57, 15–36 (1988).
- [16] A. Navarro and E.R. de los Rios, Short crack fatigue behaviour in a medium carbon steel, *Fatigue Fract. Eng. Mater. Struct.* 11, 383–396 (1988).
- [17] X.D. Li and L. Edwards, Small fatigue crack propagation in 7xxx aluminium alloys (The Open University, 1995).
- [18] X.J. Wu, Short fatigue crack behaviour of a submarine hull steel in inert and aggressive environments, Ph.D. Thesis, University Of Sheffield (January 1995).
- [19] J.W. Fash, D.F. Socie and D.L. McDowell, *Multiaxial Fatigue ASTM STP* 853, 497–513 (1985).
- [20] X.D. Li and L. Edwards, Simulation of kinetic transition from Stage I to Stage II growth for Small Fatigue Crack, submitted to *Mechanics Of Materials*.
- [21] Jack Telesman, A study of spectrum fatigue crack propagation in two aluminium alloys – II. Influence of microstructures, *Eng. Fract. Mech.* 24, 463–477 (1986).
- [22] P. Parker, *The Mechanics of Fracture and Fatigue* (Spon, 1981).
- [23] C.R. Prasad and R.K. Pandey, A composite crack profile model for CTOD determination – II. An experimental application to a small scale yielding situation, *Eng. Fract. Mech.* 24, 539–552 (1986).
- [24] C.R. Prasad and R.K. Pandey, Composite crack profile model for CTOD determination – III. An experimental application to elastic-plastic crack growth situations, *Eng. Fract. Mech.* 26, 811–824 (1987).
- [25] W.G. Reuter and W.R. Lloyd, Measurements of CTOD and CTOA around surface-crack perimeters and relationships between elastic and elastic-plastic CTOD values, *Surface-crack growth: Model, Experiments, and Structures, ASTM STP* 1060, 152–176 (1990).
- [26] S. Bhattacharya and A.N. Kumar, A new approach for CTOD evaluation in slow crack growth situation, *Eng. Fract. Mech.* 40, 1089–1103 (1991).